

Contribution from the Department of Chemistry,
University of Illinois at Chicago Circle, Chicago, Illinois 60680

Molecules with an M_4X_4 Core. VII.¹⁻⁶ Crystal and Molecular Structure of Tetrameric Triethylphosphinesilver(I) Iodide

MELVYN ROWEN CHURCHILL* and BARRY G. DEBOER

Received April 16, 1975

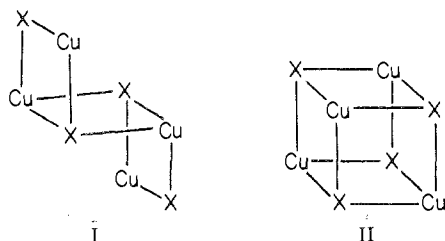
AIC50269L

The tetrameric species triethylphosphinesilver(I) iodide, $[\text{PEt}_3\text{AgI}]_4$, has been studied by single-crystal X-ray diffraction methods, in order to determine whether it has a "cubane-like" or "step" structure. This complex crystallizes from acetone in the centrosymmetric tetragonal space group $P4_2/nmc$ [D_{4h}^{15} ; No. 137] with $a = 13.7361$ (12) Å, $c = 12.0734$ (12) Å, $V = 2278.0$ (4) Å³, $\rho_{\text{obsd}} = 2.06$ (1) g cm⁻³, $\rho_{\text{calcd}} = 2.058$ g cm⁻³, and $Z = 2$. X-Ray diffraction data were collected with a Picker FACS-1 automated diffractometer using a θ - 2θ scan. All atoms were located, final discrepancy indices being $R_F = 2.99\%$ and $R_{wF} = 3.36\%$ for the 829 independent reflections which represent data complete to $2\theta = 45^\circ$ (Mo $K\alpha$ radiation). The $[\text{PEt}_3\text{AgI}]_4$ molecule lies on a site of crystallographic $42m$ (D_{2d}) symmetry and has disordered ethyl groups. The four silver and four iodine atoms, taken alternately, define the eight corners of a distorted "cubane-like" arrangement in which the two crystallographically independent Ag...I distances are 2.9184 (9) and 2.9189 (6) Å. Intramolecular Ag...Ag distances are 3.1982 (11) Å [between adjacent Ag atoms related by $\bar{4}$] and 3.2285 (12) Å [between Ag atoms related by m]; the corresponding I...I distances are 4.7676 (9) and 4.7229 (11) Å, respectively. It appears, therefore, that intramolecular iodine...iodine interactions are not so critical in determining the geometry of $[\text{PEt}_3\text{AgI}]_4$ [$I\cdots I(\text{av}) = 4.7527$ Å] as they are for the analogous copper derivative $[\text{PEt}_3\text{CuI}]_4$ [$I\cdots I = 4.3800$ (11) Å].

Introduction

We have recently determined the detailed molecular geometry of members of two complete series of tetrameric phosphinecopper(I) halide derivatives, i.e., $[\text{PPh}_3\text{CuX}]_4$ ($X = \text{Cl},^1 \text{Br},^2 \text{I}^4$) and $[\text{PEt}_3\text{CuX}]_4$ ($X = \text{Cl},^5 \text{Br},^5 \text{I}^3$); we have also carefully reexamined the species $[\text{AsEt}_3\text{CuI}]_4$,³ originally studied by Wells.^{7,8} Our results have led to two principal conclusions.

(1) The Cu_4X_4 core of a $[\text{PR}_3\text{CuX}]_4$ molecule tends preferentially to take up the "step structure", I, rather than the familiar "cubane-like" geometry, II, only when large



halogen atoms appear in conjunction with bulky phosphine ligands. Thus, $[\text{PPh}_3\text{CuBr}]_4$ ² and $[\text{PPh}_3\text{CuI}]_4$ ⁴ adopt the "step structure",⁹ while $[\text{PPh}_3\text{CuCl}]_4$,¹ $[\text{PEt}_3\text{CuI}]_4$,³ $[\text{AsEt}_3\text{CuI}]_4$,³ $[\text{PEt}_3\text{CuBr}]_4$,⁵ and $[\text{PEt}_3\text{CuCl}]_4$ ⁵ all have a "cubane-like" geometry.

(2) The detailed geometry of the four-sided Cu_2X_2 figures which constitute both I and II appears to be dictated primarily by halogen...halogen repulsions, since halogen...halogen distances are, in all cases, indistinguishable from the sum of the normal van der Waals radii (vdW).¹⁰ Thus, average I...I distances are 4.2829 Å in $[\text{PPh}_3\text{CuI}]_4$,⁴ 4.3800 Å in $[\text{PEt}_3\text{CuI}]_4$,³ and 4.4237 Å in $[\text{AsEt}_3\text{CuI}]_4$ ³ (vdW \approx 4.3 Å); average Br...Br distances are 3.9173 Å in $[\text{PPh}_3\text{CuBr}]_4$ ² and 3.9324 Å in $[\text{PEt}_3\text{CuBr}]_4$ ⁵ (vdW \approx 3.9 Å); average Cl...Cl distances are 3.5762 Å in $[\text{PPh}_3\text{CuCl}]_4$ ¹ and 3.6567 Å in $[\text{PEt}_3\text{CuCl}]_4$ ⁵ (vdW \approx 3.6 Å).

We have now extended our studies to the analogous silver(I) species in an effort to determine the systematic changes that occur as a result of an increase in the radius of the metal atom. (Shannon and Prewitt¹¹ gave $r(\text{Cu}^+) = 0.96$ Å and $r(\text{Ag}^+) = 1.26$ Å for six-coordination.)

The compound selected for our initial experiment was tetrameric triethylphosphinesilver(I) iodide.

This species was originally prepared by Mann, Wells, and Purdie,¹² who reported that "The approximate cell dimensions are: $a = 10.9$, $b = 20.8$, $c = 20.0$ Å, and for a density of 2.05 the cell contains 16 $[\text{Et}_3\text{P} \rightarrow \text{AgI}]$ components. The halvings observed are: $0kl$, k even; $h0l$, h even; $hk0$, $h + k$ even. The space group is $Pban$." Since the space group $Pban$ [D_{2h}^4 ; No. 50]^{13a} will require a tetrameric $[\text{PEt}_3\text{AgI}]_4$ molecule to lie on either an inversion center (permissible for a "step-structure") or a twofold axis (permissible for a "cubane-like" structure), we felt that an unambiguous structural assignment would be useful. However, the careful following of the synthetic procedure of Mann et al.¹² led to the formation of tetragonal crystals of $[\text{PEt}_3\text{AgI}]_4$ which had approximate unit cell dimensions $a = 13.74$ and $c = 12.07$ Å and belonged to space group $P4_2/nmc$ (vide infra). We have so far been unable to produce crystals of the type described by Mann et al.¹² and the present single-crystal X-ray diffraction study is based upon a study of the tetragonal form of $[\text{PEt}_3\text{AgI}]_4$.

As this manuscript was nearing completion, there appeared some related work by Teo and Calabrese,¹⁴ who showed that $[\text{PPh}_3\text{AgCl}]_4$ exists with a "cubane-like" Ag_4Cl_4 core, whereas $[\text{PPh}_3\text{AgI}]_4$ can be isolated in either the "cubane-like" or the "step" structure.

Experimental Section

A sample of $[\text{PEt}_3\text{AgI}]_4$ was prepared by the method of Mann et al.¹² and was recrystallized from acetone. The crystal used for the structural analysis was a rectangular parallelepiped of dimension 0.366 mm \times 0.280 mm \times 0.224 mm [distances are for (110) \rightarrow ($\bar{1}\bar{1}0$), (001) \rightarrow (00 $\bar{1}$), and ($\bar{1}\bar{1}0$) \rightarrow ($\bar{1}\bar{1}0$), respectively]. The crystal was carefully wedged into a thin-walled glass capillary, which was then flushed with nitrogen, sealed, and mounted on a eucentric goniometer.

Preliminary examination with a polarizing microscope had shown only two mutually orthogonal extinction directions. A series of precession and cone-axis photographs showed that the crystal was tetragonal with apparent $4/mmm$ (D_{4h}) Laue symmetry, provided approximate unit cell parameters, and revealed the systematic absences $hk0$ for $h + k = 2n + 1$ and hhl for $l = 2n + 1$. The centrosymmetric tetragonal space group $P4_2/nmc$ [D_{4h}^{15} ; No. 137]^{13b} is thereby indicated. The unit cell parameters and observed density dictate that, in the absence of gross disorder, the molecule must lie on a site of crystallographic $42m$ (D_{2d}) symmetry.

The crystal was transferred to our Picker FACS-1 automated diffractometer, was accurately centered, and was aligned so that [110] was coincident with the instrumental ϕ axis. As a check on the severity of the absorption problem the axial 110, 330, 440, and 660 reflections were measured (via θ - 2θ scans) at $\chi = 90^\circ$ and at 10° intervals from $\phi = 0^\circ$ to $\phi = 350^\circ$. The variations in intensity as a function of ϕ [defined by (maximum - minimum)/average] were 37.5%, 31%, 26%,

* To whom correspondence should be addressed at the Department of Chemistry, State University of New York at Buffalo, Buffalo, N.Y. 14214.

Table I. Experimental Data for the X-Ray Diffraction Study of [PEt₃AgI]₄

(A) Crystal Parameters at 19.6 (3)^o^a

Crystal system: tetragonal $Z = 2$ (tetrameric units)
 Space group: $P4_2/nmc$ [$D_{2d}h^{15}$]; Mol wt 1411.73
 No. 137]
 $a = 13.7361$ (12) Å $\rho_{\text{calc}}^b = 2.058$ g cm⁻³
 $c = 12.0734$ (12) Å $\rho_{\text{obsd}}^b = 2.06$ (1) g cm⁻³
 $V = 2278.01$ (36) Å³

(B) Measurement of Intensity Data

Radiation: Mo K α^c (50 kV/14 mA)
 Filter(s): Nb foil at counter aperture (47% transmission of Mo K α)
 Attenuators: Cu foil; successive factors of ca. 3.0; used when $I_{\text{peak}} > 10^4$ counts/sec
 Takeoff angle: 3.0^o
 Detector aperture: 3 mm wide (in 2θ) \times 4 mm high (in χ)
 Crystal-detector distance: 330 mm
 Crystal orientation: ϕ axis ca. 2.5^o from [110]
 Reflections measured: hkl for all nonnegative h, k , and l
 Maximum 2θ : 45^o
 Scan type: coupled θ (crystal)- 2θ (counter)
 Scan speed: 1.0^o/min
 Scan length: $\Delta(2\theta) = (1.10 + 0.692 \tan \theta)^\circ$, starting 0.55^o below the Mo K α_1 peak
 Background measurement: stationary crystal, stationary counter; 40 sec each at beginning and end of the 2θ scan
 Standard reflections: 3 remeasured after each 48 reflections; rms deviations (following application of an anisotropic linear decay correction)^d were 0.60% for 004, 0.86% for 400, and 0.55% for 040
 Reflections collected: 1595 reflections (two forms) which were merged to 829 symmetry-independent reflections; $R_{F^2} = 2.05\%$ for merging.

(C) Treatment of Intensity Data

Conversion to $|F_o|$ and $\sigma(|F_o|)$: as in ref 15, using an "ignorance factor" of $p = 0.03$
 Absorption coefficient: $\mu = 45.40$ cm⁻¹; maximum and minimum transmission factors were 0.4256 and 0.2911^e

^a Unit cell parameters are from a least-squares fit to the setting angles of the resolved Mo K α peaks (λ 0.709300 Å)^c of 12 reflections ($2\theta = 38$ – 44°). Maximum and root-mean-square disagreements were 0.020^o and 0.011^o, respectively. ^b Neutral buoyancy in Rohrbach's solution (BaI₂·HgI₂ in methanol-water). ^c J. A. Bearden, *Rev. Mod. Phys.*, 39, 78 (1967). ^d Data reduction was performed using the Fortran IV program RDUS2, by B. G. DeBoer. ^e Absorption corrections were carried out using the Fortran IV program DRABZ by B. G. DeBoer.

and 20.5%, respectively. When these " ϕ -scan" data were corrected for absorption, the variation of intensity with ϕ was reduced to 25.8%, 19.8%, 4.9%, and 6.9% (respectively). While the ϕ dependence of the two high-angle reflections ($2\theta(440) = 16.8^\circ$, $2\theta(660) = 25.3^\circ$) is reduced to an acceptable level, the ϕ dependence of the very strong low-angle 110 reflection ($2\theta = 4.2^\circ$) is only partly compensated for, while that of the strong 330 reflection ($2\theta = 12.6^\circ$) now occupies an intermediate position. The explanation for these discrepancies is that the strong low-angle reflections are severely affected by secondary extinction (vide infra). The effect of secondary extinction on the " ϕ -scan" data for any single reflection is equivalent to an increased absorptivity (μ) for that reflection, leading to the observed increased variability in transmission factor. The data for the weaker high-angle 440 and 660 reflections, however, confirm the validity of the absorption correction.

The crystal was now deliberately offset (by ca. 2.5^o) from its [110] direction so as to reduce the probability of multiple diffraction affecting the data. Following redetermination of the orientation matrix, intensity data for one octant of the reciprocal sphere (i.e., two equivalent forms) were collected. Data collection was carried out as described in ref 15; details of the present study are given in Table I. The intensity of the standard reflections dropped by 29% (004), 15% (400), and 20% (040) during the course of data collection; this was taken into account by applying a linear anisotropic decay correction to the entire data set. (See footnote 12 of ref 2.)

Following correction for absorption, the hkl and khl reflections were averaged.⁵ The $4/mmm$ (D_{4h}) (rather than $4/m$ or C_{4h}) Laue symmetry is confirmed by the agreement between equivalent re-

flections, the value for R_{F^2} being 2.05%, where

$$R_{F^2} = \frac{\sum |F^2 - F_{av}^2|}{\sum |F^2|}$$

There were, nevertheless, some six significant discrepancies between the intensities of hkl and khl reflections. These discrepancies are assumed to be a result of multiple diffraction, since (1) the successful solution of the structure showed that the weaker of the two "equivalent" reflections was very close to the value of $|F_c|$ in each case, (2) the affected reflections are among the weaker data, so that multiple diffraction is more likely to strengthen, rather than weaken, the reflection, (3) the hkl vector of each affected reflection may be constructed as the sum of pairs of hkl vectors belonging to the 13 most intense reflections, and (4) multiple diffraction is expected to be more effective in crystals showing substantial secondary extinction effects, as is found for this crystal. [The reflections thus affected were (giving the indices for $h < k$) 017, 023, 123, 130, 453, and 480. In each case the weaker intensity was substituted for the average intensity during the final phase of the structure solution.]

Solution and Refinement of the Structures

All calculations were performed on an IBM 370/158 computer. Programs used were as follows: LSHF (structure factor calculation and least-squares refinement, by B. G. DeBoer), FORDAP (Fourier synthesis, by A. Zalkin), STANI (distances, angles, and their esd's, by B. G. DeBoer), HAITCH (idealized positions for H atoms, by B. G. DeBoer), PLOD (least-squares planes, by B. G. DeBoer), and ORTEP (thermal ellipsoid drawings, by C. K. Johnson).

The analytical scattering factors of Cromer and Mann¹⁶ were used for neutral silver, iodine, phosphorus, and carbon. The "best floated spherical H atom" values of Stewart et al.¹⁷ were also converted to analytical form.¹⁸ The real and imaginary components of anomalous dispersion were included for all nonhydrogen atoms, using the values of Cromer and Liberman.¹⁹

The function $\sum w(|F_o| - |F_c|)^2$ (where $w = 1/\sigma^2$) was minimized during least-squares refinement. Discrepancy indices are defined as

$$R_F = \left[\frac{\sum ||F_o| - |F_c||}{\sum |F_o|} \right] \times 100 (\%)$$

$$R_{wF} = \left[\frac{\sum w(|F_o| - |F_c|)^2}{\sum w|F_o|^2} \right]^{1/2} \times 100 (\%)$$

Throughout the analysis the *second setting* of space group $P4_2/nmc$ was used.^{13b} This puts the unit cell origin at $\bar{1}$, which results in computational simplification.

The structure was solved by recognizing that the molecule must lie on a site of $\bar{4}2m$ symmetry (we chose one of Wyckoff notation "a" at $1/4, 3/4, 1/4$)^{13b} with silver, phosphorus, and iodine atoms all lying at $y = 3/4$ and arranged to give sensible intramolecular distances (we guessed values of I...I = 4.5 Å, Ag-I = 2.9 Å, and Ag-P = 2.46 Å). Several cycles of least-squares refinement of positional and thermal parameters for the heavy atoms led to $R_F = 15.1\%$ and $R_{wF} = 15.8\%$. A difference-Fourier synthesis now led to the location of all carbon atoms, but it was noted that they each had a rather diffuse profile. Full-matrix refinement of positional and anisotropic thermal parameters for all nonhydrogen atoms resulted in convergence with $R_F = 4.93\%$ and $R_{wF} = 5.84\%$. However, the resulting thermal parameters for the methylene carbon atoms were ridiculously high. A careful survey of a difference-Fourier map revealed that the methylene groups were disordered. A survey of $|F_o|$ vs. $|F_c|$ for strong low-order reflections also revealed that a secondary extinction correction would be required.

A secondary extinction parameter (c) was now included.^{20,21} It enters the equation for the corrected structure amplitude, $F_{c,cor}$, in the form

$$F_{c,cor} = F_{c,uncor} (1 + c\beta F_{c,uncor}^2)^{-1/4}$$

where

$$\beta = \frac{1 + \cos^4 2\theta}{(\sin 2\theta)(1 + \cos^2 2\theta)} \left(-\frac{d \ln T}{d\mu} \right)$$

and T is the transmission factor.

Continued refinement of positional and anisotropic thermal pa-

Table II. Final Positional Parameters for $[\text{PEt}_3\text{AgI}]_4^{a,b}$

Atom	Occup ^c	x	y	z	$B,^d \text{ \AA}^2$
Ag	1/2	0.367518 (44)	3/4	0.342759 (56)	8.312
I	1/2	0.421917 (37)	3/4	0.109091 (40)	7.238
P	1/2	0.51471 (14)	3/4	0.45557 (17)	7.506
C(1)	1/2	0.4991 (15)	0.7961 (11)	0.5969 (10)	11.45
C(2)	1/2	0.4164 (11)	3/4	0.6522 (10)	13.42
C(3A)	1/2	0.6110 (13)	0.8351 (16)	0.4065 (19)	12.61
C(3B)	1/2	0.5717 (14)	0.8637 (15)	0.4776 (15)	12.50
C(4)	1	0.5897 (8)	0.9215 (8)	0.3666 (7)	14.35
H(1)	1/2	0.4885	0.8644	0.5939	16.9 (46)
H(1')	1/2	0.5566	0.7831	0.6382	
H(2)	1/2	0.4095	0.7750	0.7251	
H(2')	1/2	0.4269	0.6817	0.6554	15.4 (28)
H(2'')	1/2	0.3588	0.7630	0.6111	
H(3A)	1/2	0.6505	0.8483	0.4693	
H(3A')	1/2	0.6485	0.8019	0.3522	19.5 (86)
H(3B)	1/2	0.6339	0.8521	0.5091	
H(3B')	1/2	0.5336	0.9015	0.5272	
H(4A)	1/2	0.6474	0.9558	0.3477	14.5 (35)
H(4A')	1/2	0.5535	0.9581	0.4191	
H(4A'')	1/2	0.5515	0.9117	0.3020	
H(4B)	1/2	0.6213	0.9819	0.3797	26.4 (37)
H(4B')	1/2	0.6277	0.8835	0.3170	
H(4B'')	1/2	0.5274	0.9329	0.3351	

^a All coordinates refer to the second setting of space group $P4_2/nmc$ —i.e., origin at $\bar{1}$. ^b Esd's, shown in parentheses, are right adjusted to the last digit of the preceding number. They are derived from the inverse of the final least-squares matrix. ^c The occupancy is the multiplier to the atom's contribution to F_o using the general expression for space group $P4_2/nmc$, which has 16 equipoints. It will take a value of 1/2 both for atoms which lie on the mirror plane at $y = 3/4$ and for atoms which are involved in the twofold disorder (i.e., methylene groups and methyl hydrogens). ^d For nonhydrogen atoms, the "equivalent isotropic thermal parameter" is given. For the full anisotropic expression, see Table III.

Table III. Anisotropic Thermal Parameters for $[\text{PEt}_3\text{AgI}]_4^a$

Atom	B_{11}	B_{22}	B_{33}	B_{12}	B_{13}	B_{23}	$\langle U \rangle^b$
Ag	6.42 (3)	9.85 (4)	8.66 (4)	0	-0.99 (3)	0	0.277, 0.338, 0.353
I	6.78 (3)	7.24 (3)	7.70 (3)	0	1.62 (2)	0	0.265, 0.303, 0.336
P	6.24 (9)	7.84 (11)	8.43 (11)	0	-0.90 (8)	0	0.274, 0.315, 0.333
C(1)	13.7 (10)	11.5 (10)	9.1 (7)	-0.2 (8)	-1.4 (9)	-0.1 (6)	0.33, 0.38, 0.42
C(2)	13.7 (10)	16.8 (11)	9.8 (7)	0	0.3 (7)	0	0.35, 0.42, 0.46
C(3A)	6.9 (9)	12.3 (13)	18.6 (18)	-2.5 (8)	-2.2 (9)	4.9 (13)	0.27, 0.35, 0.53
C(3B)	10.7 (13)	14.9 (14)	11.9 (11)	-5.9 (10)	1.0 (9)	-3.4 (11)	0.28, 0.37, 0.51
C(4)	16.2 (8)	12.0 (7)	14.9 (7)	-5.9 (6)	-1.0 (6)	1.0 (5)	0.32, 0.43, 0.51

^a These anisotropic thermal parameters have units of \AA^2 and are analogous to the normal isotropic thermal parameters, entering the expression for F_o in the form $\exp[-0.25\{(h^2B_{11} + k^2B_{22} + 2hkB_{12})a^{*2} + l^2B_{33}c^{*2} + (2hlB_{13} + 2klB_{23})a^*c^*\}]$. ^b These values are the root-mean-square amplitudes of vibration (in \AA) of the atoms along the principal axes of their ellipsoids. For orientations, see Figures 1 and 2.

rameters for all atoms (with the methylene carbon atoms now correctly assigned to their disordered positions) led to convergence with $R_F = 3.37\%$ and $R_{WF} = 5.20\%$. There were still, however, some substantial statistical differences between $|F_o|$ and $|F_c|$, the most significant being $\Delta F = 28.9\sigma$ for 012. We decided, therefore, to include all hydrogen atoms in calculated positions (based upon $d(\text{C-H}) = 0.95 \text{\AA}$,²² regular tetrahedral stereochemistry about carbon, and a perfectly staggered conformation for each ethyl group).

Continued refinement, with shifts of hydrogen atoms set equal to the shifts of their attached carbon atoms and with an overall isotropic thermal parameter for all hydrogen atoms attached to a given carbon atom, led to final convergence with $R_F = 2.99\%$ and $R_{WF} = 3.36\%$. The largest ΔF values were now only 6.1σ for 176 and 4.7σ for 9,11,0. The inclusion of hydrogen atoms in calculated positions thus leads to a highly significant improvement in the model.

The largest shifts during the final cycle of refinement were 0.025σ for a "heavy atom" parameter, 0.29σ for a carbon atom parameter, and 0.44σ for an isotropic (hydrogen) thermal parameter. The "goodness of fit", defined by $[\sum w(|F_o| - |F_c|)^2 / (m - n)]^{1/2}$ was 1.303 e, where m (the number of observations) was 829, n (the number of variables) was 67, and $m:n = 12.37:1$. The final value for the secondary extinction parameter was $c = 0.97 (19) \times 10^{-6} \text{ mm}^{-1} \text{ e}^{-2}$. The highest features on a final difference Fourier synthesis were peaks of height 0.34 e \AA^{-3} (at 0.25, 0.75, 0.35) and 0.33 e \AA^{-3} (at 0.41, 0.81, 0.35). The correctness of the refined structure is therefore confirmed.

A table of observed and calculated structure factor amplitudes may be obtained. [See paragraph at end of paper regarding supplementary material.]

Table IV. Interatomic Distances (\AA) with Esd's for $[\text{PEt}_3\text{AgI}]_4^{a-c}$

Atoms	Dist	Atoms	Dist
Ag ··· Ag [I] ^d	3.2285 (12)	Ag-P	2.4379 (19)
Ag ··· Ag [II] ^d	3.1982 (11)	P-C(1)	1.833 (12)
Ag ··· Ag [III] ^d	3.1982 (11)	P-C(3A)	1.862 (18)
Ag-I	2.9184 (9)	P-C(3B)	1.766 (17)
Ag-I [II] ^d	2.9189 (6)	C(1)-C(2)	1.462 (19)
Ag-I [III] ^d	2.9189 (6)	C(3A)-C(4)	1.314 (20)
I ··· I [I] ^d	4.7229 (11)	C(3B)-C(4)	1.577 (17)
I ··· I [II] ^d	4.7676 (9)	C(1) ··· C(1) [IV] ^d	1.266 (29)
I ··· I [III] ^d	4.7676 (9)	C(3A) ··· C(3B)	1.087 (23)

^a Esd's were calculated from the final full positional correlation matrix, using the Fortran IV program STANI, by B. G. DeBoer. Errors in the unit cell parameters are also included. ^b Bond lengths have not been corrected for any possible systematic errors due to thermal motion. ^c The molecule has precise $42m(D_{2d})$ symmetry, being centered on the special position $(1/4, 3/4, 1/4)$ of space group $P4_2/nmc$ (second setting, with $\bar{1}$ as origin). ^d Transformations are as follows: [I] = $(1/2 - x, y, z)$; [II] = $(1 - y, 1 - x, 1/2 - z)$; [III] = $(1 - y, 1/2 + x, 1/2 - z)$; [IV] = $(x, 1/2 - y, z)$.

Positional parameters are collected in Table II; anisotropic thermal parameters are shown in Table III.

The Molecular Structure

The tetrameric $[\text{PEt}_3\text{AgI}]_4$ molecules lie on sites of $42m(D_{2d})$ symmetry; the crystallographic asymmetric unit thus consists of one-eighth of the molecule. The individual tet-

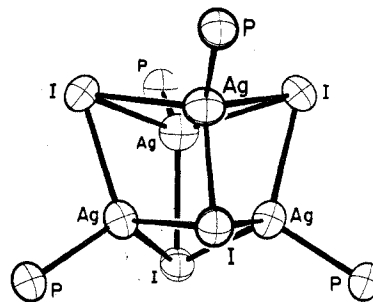
Table V. Intramolecular Angles (Deg) with Esd's for [PEt₃AgI]₄^a

Atoms	Angle	Atoms	Angle
I-Ag-I[II]	109.52 (2)	C(1)-P-C(1)[IV]	40.4 (9)
I-Ag-I[III]	109.52 (2)	C(1)-P-C(3A)	99.4 (9)
I[II]-Ag-I[III]	108.00 (2)	C(1)-P-C(3A)[IV]	126.6 (8)
P-Ag-I	109.13 (6)	C(1)-P-C(3B)	66.8 (8)
P-Ag-I[III]	110.33 (3)	C(1)-P-C(3B)[IV]	102.5 (8)
P-Ag-I[III]	110.33 (3)	C(3A)-P-C(3A)[IV]	77.8 (15)
Ag-I-Ag[II]	66.44 (2)	C(3A)-P-C(3B)	34.8 (7)
Ag-I-Ag[III]	66.44 (2)	C(3A)-P-C(3B)[IV]	106.7 (11)
Ag[II]-I-Ag[III]	67.15 (2)	C(3B)-P-C(3B)[IV]	124.2 (16)
Ag-P-C(1)	115.1 (6)	P-C(1)-C(2)	111.5 (12)
Ag-P-C(3A)	114.3 (6)	P-C(3A)-C(4)	121.7 (14)
Ag-P-C(3B)	116.8 (7)	P-C(3B)-C(4)	112.8 (10)

^a See footnotes to Table IV.

ramer units are mutually separated by van der Waals distances, there being no abnormally short intermolecular contacts.

The central P₄Ag₄I₄ portion of the molecule is illustrated in Figure 1. The entire molecule (barring the hydrogen atoms, which are omitted for the sake of clarity), as viewed down its crystallographic $\bar{4}$ (S₄) axis, is shown in Figure 2. Interatomic distances with their estimated standard deviations (esd's) are listed in Table IV; bond angles and their esd's are collected in Table V.

Figure 1. The P₄Ag₄I₄ core of the [PEt₃AgI]₄ molecule (ORTEP diagram, 30% probability envelopes).

The Ag₄I₄ core of the [PEt₃AgI]₄ molecule defines a "cubane-like" figure. The six four-membered faces of the "cube" are each severely distorted from planarity. Dihedral angles within the Ag₂I₂ faces are as follows. (i) For the four equivalent faces related by operations of the $\bar{4}$ axis, the dihedral angle across the I...I vector is 143.43° and that across the Ag...Ag vector is 155.00°. (ii) For the two equivalent faces which are perpendicular to the $\bar{4}$ axis, the dihedral angle across the I...I vector is 140.39° while that across the Ag...Ag vector is 152.34°. [For details of these planes, see Table VI.]

Despite the considerable difference between the lengths of the crystallographic *a* and *c* axes of the [PEt₃AgI]₄ crystal

Table VI. Planes and Dihedral Angles for [PEt₃AgI]₄^{a,b}

Atom	Dev, Å	Atom	Dev, Å
Plane I: 0.58319X + 0.79752Y + 0.15447Z = 11.7994			
Ag(x, y, z)*	0.000	I(1 - y, 1/2 + x, 1/2 - z)	1.032
Ag(1 - y, 1/2 + x, 1/2 - z)*	0.000	Cent ^c	-1.114
I(x, y, z)*	0.000		
Plane II: 0.79752X + 0.58319Y - 0.15447Z = 9.3949			
Ag(x, y, z)*	0.000	I(x, y, z)	1.032
Ag(1 - y, 1/2 + x, 1/2 - z)*	0.000	Cent ^c	-1.114
I(1 - y, 1/2 + x, 1/2 - z)*	0.000		
Plane III: 0.82973X + 0.51308Y + 0.21977Z = 10.3839			
I(x, y, z)*	0.000	Ag(1 - y, 1/2 + x, 1/2 - z)	-1.003
I(1 - y, 1/2 + x, 1/2 - z)*	0.000	Cent ^c	-1.586
Ag(x, y, z)*	0.000		
Plane IV: 0.51308Y + 0.82973X - 0.21977Z = 11.2320			
I(x, y, z)*	0.000	Ag(x, y, z)	-1.003
I(1 - y, 1/2 + x, 1/2 - z)*	0.000	Cent ^c	-1.586
Ag(1 - y, 1/2 + x, 1/2 - z)*	0.000		
Plane V: -0.23904Y + 0.97101Z = 1.5557			
Ag(x, y, z)*	0.000	I(1 - y, 1 - x, 1/2 - z)	1.129
Ag(1/2 - x, y, z)*	0.000	Cent ^c	-1.087
I(1 - y, 1/2 + x, 1/2 - z)*	0.000		
Plane VI: 0.23904Y + 0.97101Z = 6.4809			
Ag(x, y, z)*	0.000	I(1 - y, 1/2 + x, 1/2 - z)	1.129
Ag(1/2 - x, y, z)*	0.000	Cent ^c	-1.601
I(1 - y, 1 - x, 1/2 - z)*	0.000		
Plane VII: 0.33883X + 0.94085Z = 5.6040			
I(1 - y, 1/2 + x, 1/2 - z)*	0.000	Ag(1/2 - x, y, z)	-1.094
I(1 - y, 1 - x, 1/2 - z)*	0.000	Cent ^c	-1.601
Ag(x, y, z)*	0.000		
Plane VIII: -0.33883X + 0.94085Z = 3.2769			
I(1 - y, 1/2 + x, 1/2 - z)	0.000	Ag(x, y, z)	-1.094
I(1 - y, 1 - x, 1/2 - z)*	0.000	Cent ^c	-1.601
Ag(1/2 - x, y, z)*	0.000		
Dihedral Angles, Deg			
(A) Across Ag...Ag		(B) Across I...I	
I-II	155.00	III-IV	143.43
V-VI	152.34	VII-VIII	140.39

^a Cartesian coordinates ($X = ax, Y = ay, Z = cz$). Only atoms marked with an asterisk were used in calculating the planes. ^b Calculations were performed using the program PLOD, by B. G. DeBoer. ^c Cent is the centroid of the molecule (fractional coordinates $x = 1/4, y = 3/4, z = 1/4$).

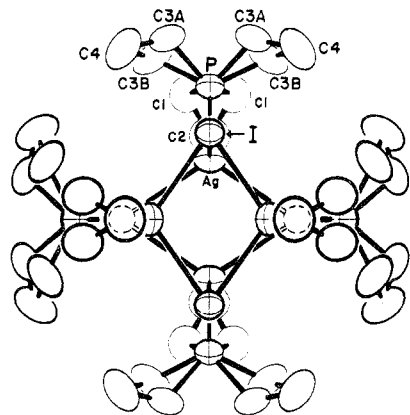


Figure 2. The $[\text{PEt}_3\text{AgI}]_4$ molecule viewed along its $\bar{4}(S_4)$ axis. (The x axis is vertical, the y axis is horizontal, and the $\bar{4}$ axis defines the z direction.)

[$a = 13.7361 \text{ \AA}$, $c = 12.0734 \text{ \AA}$, difference (%) = $100(a - c)/\frac{1}{2}(a + c) = 12.88\%$], the tetragonal distortion of the Ag_4I_4 core from perfect T_d symmetry is slight, although it is statistically significant.

Since the four silver atoms are crystallographically equivalent, we need to consider the geometry about only one. The silver-iodine bond distances are 2.9184 (9), 2.9189 (6), and 2.9189 (6) \AA , averaging $2.9187 \pm 0.0003 \text{ \AA}$.²³ The nonbonding silver...silver distances show rather greater variations, individual values being 3.1982 (11), 3.1982 (11) and 3.2285 (12) \AA , with a mean value of $3.2083 \pm 0.0175 \text{ \AA}$.²³

Intramolecular iodine...iodine distances are 4.7229 (11), 4.7676 (9), and 4.7676 (9) \AA . The mean value of $4.7527 \pm 0.0258 \text{ \AA}$ ²³ is considerably greater than the accepted van der Waals distance of ca. 4.3 \AA for $\text{I}\cdots\text{I}$ ¹⁰ and is almost 0.4 \AA greater than the $\text{I}\cdots\text{I}$ distance of 4.3800 (11) \AA found in the closely related copper complex $[\text{PEt}_3\text{CuI}]_4$.³ This immediately suggests that intramolecular halogen...halogen repulsions are nowhere nearly as important in $[\text{PR}_3\text{AgX}]_4$ species as they are in $[\text{PR}_3\text{CuX}]_4$ species (cf. ref 4 and 5, which contain detailed analyses of $[\text{PPh}_3\text{CuX}]_4$ and $[\text{PEt}_3\text{CuX}]_4$ molecules ($X = \text{Cl}, \text{Br}, \text{I}$), respectively).

In agreement with this suggestion we find that the Ag_4I_4 core is less rigid than the Cu_4I_4 core—this manifests itself in numerically higher values for the thermal parameters of all atoms within the Ag_4I_4 core of $[\text{PEt}_3\text{AgI}]_4$ relative to those in the Cu_4I_4 core of the isostructural compound $[\text{PEt}_3\text{CuI}]_4$ (see Table VII). Note that the thermal parameters of all atoms are high—this appears to be general among species with a “cubane-like” structure and may be interpreted as evidence against there being any direct metal-metal bonding.

Angles within the cubane-like Ag_4I_4 core of the present molecule lie in the following ranges: $\text{I}-\text{Ag}-\text{I} = 108.00$ (2)– 109.52 (2) $^\circ$ [average 109.01° —i.e., very close to the regular tetrahedral value of 109.47°] and $\text{Ag}-\text{I}-\text{Ag} = 66.44$ (2)– 67.15 (2) $^\circ$ [average 66.68°]. These are surprisingly similar to the values found within the $[\text{PEt}_3\text{CuI}]_4$ molecule³—viz., $\text{I}-\text{Cu}-\text{I} = 109.38$ (4) $^\circ$ and $\text{Cu}-\text{I}-\text{Cu} = 66.10$ (4) $^\circ$.

The silver-phosphorus bonds are 2.4379 (19) \AA in length—i.e., some 0.18 \AA longer than the copper-phosphorus linkages in $[\text{PEt}_3\text{CuI}]_4$.³ The geometry of the triethylphosphine ligand is as expected, although the accuracy of location of the carbon atoms is relatively poor, both as a result of their small contribution to the overall structure factor amplitudes [there are four silver ($Z = 47$), four iodine ($Z = 53$), and four phosphorus ($Z = 15$) atoms in the molecule] and as a result of the disorder of the ethyl groups (see Figure 2). The $\text{Ag}-\text{P}-\text{C}$ angles range from 114.3 (6) to 116.8 (7) $^\circ$, averaging 115.4° . The triethylphosphine ligand has two rotational conformations about the $\text{Ag}-\text{P}$ bonds; the angle between the two conformers

Table VII. Comparison of Data on $[\text{PEt}_3\text{AgI}]_4$ with Those on $[\text{PEt}_3\text{CuI}]_4$

	M = Ag	M = Cu	Δ^a
Molecular symmetry	$\bar{4}2m (D_{2d})$	$\bar{4}3m (T_d)$	
a axis, \AA	13.7361 (12)	13.0241 (11)	
b axis, \AA	13.7361 (12)	13.0241 (11)	
c axis, \AA	12.0734 (12)	13.0241 (11)	
V , \AA^3	2278.0 (4)	2209.2 (3)	+68.8
$B(\text{M})$, \AA^2	8.312	5.68	+2.63
$B(\text{I})$, \AA^2	7.238	5.64	+1.60
$B(\text{P})$, \AA^2	7.506	6.03	+1.48
$\text{M}\cdots\text{M}$, \AA	3.2083 ^b	2.9272 (20)	+0.2811
$\text{I}\cdots\text{I}$, \AA	4.7527 ^b	4.3800 (11)	+0.3727
$\text{M}-\text{I}$, \AA	2.9187 ^b	2.6837 (13)	+0.2350
$\text{M}-\text{P}$, \AA	2.4379 (19)	2.2538 (27)	+0.1841
$\text{I}-\text{M}-\text{I}$, deg	109.01 ^b	109.38 (4)	-0.37
$\text{P}-\text{M}-\text{I}$, deg	109.93 ^b	109.56 (8)	+0.37
$\text{M}-\text{I}-\text{M}$, deg	66.68 ^b	66.10 (4)	+0.58
$\text{M}-\text{P}-\text{C}$, deg	115.4 ^b	117.0 (10)	-1.6

^a $\Delta = [(\text{value for Ag complex}) - (\text{value for Cu complex})]$.

^b These values are each the average of two or more independent measurements. (For individual values and their esd's, see Tables IV and V.)

is $\sim 37.6^\circ$ (the two independent measurements are $\text{C}(1)-\text{P}-\text{C}(1)[\text{IV}]^{24} = 40.4$ (9) $^\circ$ and $\text{C}(3\text{A})-\text{P}-\text{C}(3\text{B}) = 34.8$ (7) $^\circ$). The atoms $\text{C}(1)$, $\text{C}(3\text{A})$, and $\text{C}(3\text{B})[\text{IV}]^{24}$ define the methylene carbons of one conformer, while atoms $\text{C}(1)[\text{IV}]$, $\text{C}(3\text{A})[\text{IV}]$, and $\text{C}(3\text{B})$ define those of the other conformer. $\text{C}-\text{P}-\text{C}$ angles are $\text{C}(1)-\text{P}-\text{C}(3\text{A}) = 99.4$ (9) $^\circ$, $\text{C}(3\text{A})-\text{P}-\text{C}(3\text{B})[\text{IV}] = 106.7$ (11) $^\circ$, and $\text{C}(3\text{B})[\text{IV}]-\text{P}-\text{C}(1) = 102.5$ (8) $^\circ$ [average 102.9°]. The reduction of $\text{C}-\text{P}-\text{C}$ angles in $\text{M}-\text{PR}_3$ species from a regular tetrahedral value is a well-established phenomenon and has been documented previously by Churchill and O'Brien.²⁵ Carbon-carbon distances lie in the range 1.314 (20)–1.577 (17) \AA [average 1.454 \AA] and the separation between disordered methylene groups is given by $\text{C}(1)\cdots\text{C}(1)[\text{IV}] = 1.266$ (29) \AA and $\text{C}(3\text{A})\cdots\text{C}(3\text{B}) = 1.087$ (23) \AA . Finally, we note that a similar pattern of disordered methylene groups and methyl hydrogen atoms is found in the related species $[\text{PEt}_3\text{CuI}]_4$,³ $[\text{AsEt}_3\text{CuI}]_4$,³ $[\text{PEt}_3\text{CuBr}]_4$,⁵ and $[\text{PEt}_3\text{CuCl}]_4$.⁵

Conclusions

The $[\text{PEt}_3\text{AgI}]_4$ molecule takes up a “cubane-like” geometry, as does $[\text{PEt}_3\text{CuI}]_4$. However, the intramolecular $\text{I}\cdots\text{I}$ contacts are about 0.4 \AA longer in the silver derivative than they are in the copper species. It would appear, then, that the larger second-row transition metal ion leads to an overall expansion of the “cubane-like” cage and leads to reduced intramolecular repulsions. The “cubane-like” structure is thus not as likely to be transformed into the “step” structure as a result of such repulsions. [We have noted previously⁴ that, in the absence of such phenomena as chelate-enforced configurations, “...the step structure is favored over the cubane-like arrangement in $[\text{PR}_3\text{CuX}]_4$ tetramers only when both bulky phosphine ligands and large halogen atoms are present.”

The increased openness of the Ag_4I_4 (vis à vis Cu_4I_4) framework leads one to believe that the step structure will occur preferentially to the cubane-like structure less frequently in $[\text{PR}_3\text{AgX}]_4$ systems than it does in $[\text{PR}_3\text{CuX}]_4$ species. In support of this we note that both cubane-like and step-like isomers of $[\text{PPh}_3\text{AgI}]_4$ have been reported,¹⁴ while only the step-like isomer of $[\text{PPh}_3\text{CuI}]_4$ is known.⁴

Acknowledgment. We thank Mr. Stephen J. Mendak for experimental assistance. This work was made possible by financial support from the National Science Foundation (Grant GP-42724, to M.R.C.) and by a generous allocation of time on the IBM 370/158 computer at the Computing Center of the University of Illinois at Chicago Circle.

Registry No. [PEt₃AgI]₄, 55853-47-9.

Supplementary Material Available. A listing of structure factor amplitudes will appear following these pages in the microfilm edition of this volume of the journal. Photocopies of the supplementary material from this paper only or microfiche (105 × 148 mm, 24× reduction, negatives) containing all of the supplementary material for the papers in this issue may be obtained from the Journals Department, American Chemical Society, 1155 16th St., N.W., Washington, D.C. 20036. Remit check or money order for \$4.00 for photocopy or \$2.50 for microfiche, referring to code number AIC50269L-10-75.

References and Notes

- (1) Part I: M. R. Churchill and K. L. Kalra, *Inorg. Chem.*, **13**, 1065 (1974).
- (2) Part II: M. R. Churchill and K. L. Kalra, *Inorg. Chem.*, **13**, 1427 (1974).
- (3) Part III: M. R. Churchill and K. L. Kalra, *Inorg. Chem.*, **13**, 1899 (1974).
- (4) Part IV: M. R. Churchill, B. G. DeBoer, and D. J. Donovan, *Inorg. Chem.*, **14**, 617 (1975).
- (5) Part V: M. R. Churchill, B. G. DeBoer, and S. J. Mendak, *Inorg. Chem.*, **14**, 2041 (1975).
- (6) Part VI: M. R. Churchill, B. G. DeBoer, and S. J. Mendak, preceding paper in this issue.
- (7) A. F. Wells, *Z. Kristallogr., Kristallgeom., Kristallphys., Kristallchem.*, **94**, 447 (1936).
- (8) F. G. Mann, D. Purdie, and A. F. Wells, *J. Chem. Soc.*, 1503 (1936).
- (9) All halides of the form (PPh₂CH₂Ph₂P)₂Cu₄X₄ also have a "step-like" Cu₄X₄ core. We have excluded them from our discussion because of the possible complications caused by the rigid chelating diphosphine ligand. References are as follows: (PPh₂CH₂Ph₂P)₂Cu₄I₄, N. Marsich, G. Nardin, and L. Randaccio, *J. Am. Chem. Soc.*, **95**, 4053 (1973); (PPh₂CH₂Ph₂P)₂Cu₄Cl₄, G. Nardin and L. Randaccio, *Acta Crystallogr.*,

- Sect. B*, **30**, 1377 (1974); (PPh₂CH₂Ph₂P)₂Cu₄Br₄ and (PPh₂CH₂Ph₂P)₂Cu₄I₄, A. Camus, G. Nardin, and L. Randaccio, *Inorg. Chim. Acta*, **12**, 23 (1975).
- (10) L. Pauling, "The Nature of the Chemical Bond", 3rd ed, Cornell University Press, Ithaca, N.Y., 1960, p 260.
 - (11) R. D. Shannon and C. T. Prewitt, *Acta Crystallogr., Sect. B*, **25**, 925 (1969).
 - (12) F. G. Mann, A. F. Wells, and D. Purdie, *J. Chem. Soc.*, 1828 (1937).
 - (13) "International Tables for X-Ray Crystallography", Vol. 1, 2nd ed, Kynoch Press, Birmingham, England, 1965: (a) p 137, (b) pp 237-238.
 - (14) B.-K. Teo and J. C. Calabrese, *J. Am. Chem. Soc.*, **97**, 1256 (1975).
 - (15) M. R. Churchill and B. G. DeBoer, *Inorg. Chem.*, **12**, 525 (1973).
 - (16) D. T. Cromer and J. B. Mann, *Acta Crystallogr., Sect. A*, **24**, 321 (1968).
 - (17) R. F. Stewart, E. R. Davidson, and W. T. Simpson, *J. Chem. Phys.*, **42**, 3175 (1965); see Table II on p 3178.
 - (18) See footnote 14 of ref 4.
 - (19) D. T. Cromer and D. Liberman, *J. Chem. Phys.*, **53**, 1891 (1970).
 - (20) W. H. Zachariasen, *Acta Crystallogr.*, **16**, 1139 (1963); **23**, 558 (1967).
 - (21) A. C. Larson in "Crystallographic Computing", F. R. Ahmed, Ed., Munksgaard, Copenhagen, 1970, p 291 ff.
 - (22) M. R. Churchill, *Inorg. Chem.*, **12**, 1213 (1973).
 - (23) Esd's on average bond lengths are calculated by the "scatter" equation (see below) and appear in the text preceded by "±" to distinguish them from esd's on individual bond lengths (which are given in parentheses).

$$\sigma(\text{of average}) = \left[\frac{\sum_{i=1}^{i=N} (\chi_i - \bar{\chi})^2}{(N-1)} \right]^{1/2}$$

Here χ_i is the i th value and $\bar{\chi}$ is the mean of the N values.

- (24) The transformations of atoms from the basic asymmetric unit are shown as bracketed Roman numerals. The key to these transformations is given as footnote d to Table IV.
- (25) M. R. Churchill and T. A. O'Brien, *J. Chem. Soc. A*, 2970 (1968); see, especially, Table 7.

Contribution from the Department of Chemistry,
The University of Texas at Austin, Austin, Texas 78712

Crystal and Molecular Structure of a 1:2 Cyclobutadieneiron Tricarbonyl-Dimethyl Maleate Photoadduct

PAUL E. RILEY and RAYMOND E. DAVIS*

Received April 15, 1975

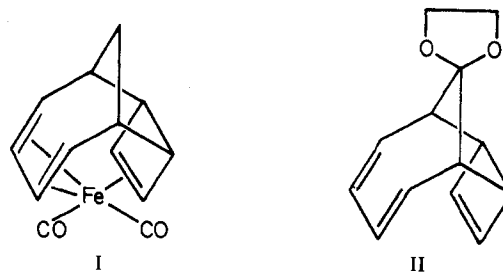
AIC50264O

The crystal structure of C₁₆H₂₀O₈Fe(CO)₃, a 1:2 cyclobutadieneiron tricarbonyl-dimethyl maleate photoadduct, has been determined by single-crystal X-ray diffraction techniques using three-dimensional data gathered by counter methods. Crystals are pale yellow plates, of orthorhombic space group *P*2₁2₁2, with unit cell parameters at 23 (1)° of $a = 15.646$ (2), $b = 23.941$ (2), and $c = 11.033$ (1) Å. A calculated density of 1.550 g cm⁻³ for eight formula units of C₁₆H₂₀O₈Fe(CO)₃ per cell agrees with the measured value of 1.551 g cm⁻³. The two discrete molecules of the asymmetric unit are related by a pseudo-*b*-glide plane at $x \approx 0.26$, approximating space group *Pbca*. Each Fe atom is coordinated to a distorted octahedron of carbon atoms—three CO molecules which form a Fe(CO)₃ moiety with nearly C_{3v} symmetry, two C(sp³) atoms from two dimethyl maleate molecules, and the π -bonding C=C group of a cyclobutene ring. Both maleate residues are bonded to adjacent cyclobutene sp³ carbon atoms by one of their former olefinic maleate carbon atoms and then to Fe through their other olefinic carbon. In terms of the Dewar-Chartt description of metal-alkene bonding, the cyclobutene ring has been twisted by ca. 45° with respect to the Fe $d\pi$ -donor orbitals, a consequence of the formation of the two-carbon bridges between the Fe atom and the sp³ carbon atoms of the ring. Hence the alkene π^* -acceptor orbitals are unable to achieve as strong an interaction as usual with the π orbitals of Fe. This is reflected by the long Fe—(C=C) π bond (mean Fe—C distance 2.26 (2) Å) and by the observed C=C bond length of 1.35 (1) Å, a value which is virtually that of a normal alkene bond. Full-matrix least-squares refinement has converged with a weighted *R* index (on $|F|$) of 0.051 for the 2779 reflections with $I_0 > 2.0\sigma(I_0)$.

Introduction

The utility in organic synthesis of molecules containing metal carbonyl groups coordinated to unsaturated organic moieties has been amply demonstrated.¹ In a continuing effort to characterize molecular cyclobutadiene (C₄H₄) and to extend the synthetic usefulness of this extremely reactive entity, Pettit and coworkers²⁻⁴ have carried out a variety of reactions with C₄H₄Fe(CO)₃—an unsaturated iron carbonyl complex which may be considered as a stabilized source of cyclobutadiene for subsequent synthetic use. Thus it has been shown that C₄H₄Fe(CO)₃ adds to cycloheptatriene to form I⁵ and to the ethylene ketal of tropone to give a complex which upon

subsequent degradation (i.e., loss of Fe(CO)₃) yields II.⁶ If



C₄H₄Fe(CO)₃ is treated with dimethyl maleate or dimethyl